Sandra S. Donato[1,2]
Virginia Chu[1]
Duarte M. F. Prazeres[2,3]
Joao P. Conde[1,3]

[1]INESC Microsistemas e Nanotecnologias and IN-Institute of Nanoscience and Nanotechnology, Lisbon, Portugal
[2]IBB – Institute for Biotechnology and Bioengineering, Centre for Biological and Chemical Engineering, Instituto Superior Técnico, Technical University of Lisbon, Lisbon, Portugal
[3]Department of Bioengineering, Instituto Superior Técnico, Technical University of Lisbon, Lisbon, Portugal

Received May 30, 2012
Revised October 12, 2012
Accepted October 17, 2012

Research Article

Metabolic viability of *Escherichia coli* trapped by dielectrophoresis in microfluidics

The spatial and temporal control of biological species is essential in complex microfluidic biosystems. In addition, if the biological species is a cell, microfluidic handling must ensure that the cell's metabolic viability is maintained. The use of DEP for cell manipulation in microfluidics has many advantages because it is remote and fast, and the voltages required for cell trapping scale well with miniaturization. In this paper, the conditions for bacterial cell (*Escherichia coli*) trapping using a quadrupole electrode configuration in a PDMS microfluidic channel were developed both for stagnant and for in-flow fluidic situations. The effect of the electrical conductivity of the fluid, the applied electric field and frequency, and the fluid-flow velocity were studied. A dynamic exchange between captured and free-flowing cells during DEP trapping was demonstrated. The metabolic activity of trapped cells was confirmed by using *E. coli* cells genetically engineered to express green fluorescent protein under the control of an inducible promoter. Noninduced cells trapped by negative DEP and positive DEP were able to express green fluorescent protein minutes after the inducer was inserted in the microchannel system immediately after DEP trapping. Longer times of trapping prior to exposure to the inducer indicated first a degradation of the cell metabolic activity and finally cell death.

Keywords:
Dielectrophoresis / *Escherichia coli* / Fluorescence microscopy / Metabolic viability / Microfluidics
DOI 10.1002/elps.201200292

Additional supporting information may be found in the online version of this article at the publisher's web-site

1 Introduction

Microorganisms such as bacteria are present in our everyday life requiring careful control of their presence and concentration. More recently, the concept of using microorganisms and their biomolecular machinery as live sensors to monitor environmental conditions has been proposed [1, 2]. Traditional microbiology techniques are generally time-consuming and labor-intensive, and thus cannot provide immediate results or be used for continuous monitoring. Analyses performed in micro-environments such as lab-on-a-chip devices, in which the small characteristic dimensions decrease mass and thermal diffusion times, have become an important alternative [3–6]. Microfluidic devices have had an impact in fields such as food and water control [7], biological and medical studies [8,9], DNA and protein manipulation [10], and environmental monitoring [11]. The ability to accurately control and manipulate bacteria cells in a microfluidic environment is thus essential to enable a high-throughput, faster, and more accurate analysis using live bacterial sensors [12]. The great majority of the biological tests to be performed in a microfluidic environment would require processes such as placing and patterning the biological entities with micrometric precision into desired locations on the chip, as well as detecting and sorting these entities according to their different characteristics. DEP has been reported as presenting potential applications for bioparticle separation [13–15] and patterning [16].

DEP was first described by Pohl [17] as the motion of a dielectric particle in the presence of a nonuniform electric field. The effect is based on the differences of electrical polarizability between the particles and the surrounding medium. The theory of DEP is described in a wide range of publications [16–18]. DEP forces, acting on a spherical particle, can be described by Eq. (1):

$$F_{\mathrm{DEP}}(r) = 2\pi\varepsilon_{\mathrm{m}}\varepsilon_0 R^3 [F_{\mathrm{CM}}(\omega)] \nabla E^2(r) \quad (1)$$

Correspondence: Professor Joao P. Conde, INESC Microsistemas e Nanotecnologias and IN-Institute of Nanoscience and Nanotechnology, Technical University of Lisbon, Rua Alves Redol, 9, Lisbon 1000-029, Portugal
E-mail: joao.conde@ist.utl.pt
Fax: +351-21-3145843

Abbreviations: GFP, green fluorescence protein; **nDEP**, negative DEP; **pDEP**, positive DEP

Colour Online: See the article online to view Figs. 1–5 in colour.

$$F_{CM} = \frac{\varepsilon_p^* - \varepsilon_m^*}{\varepsilon_p^* + 2\varepsilon_m^*} \quad (2)$$

In Eq. (1), the Clausius–Mossotti factor, $F_{CM,}$ defined in Eq. (2), denotes the real part of the Maxwell–Wagner relaxation, the complex permittivity, ε^*, is defined as $\varepsilon^* = \varepsilon - \frac{\sigma}{\omega} j$, where ε is the relative permittivity, σ is the electric conductivity, the subscripts p and m refer to particle and medium, respectively, ω is the angular frequency of the electric field E, $\nabla$is the gradient operator, and $j = \sqrt{-1}$. The F_{CM} describes the frequency dependence of the effective polarizability. The DEP force depends upon the magnitude and sign of the F_{CM} as well as the cubic cell radius, R^3. It is possible to distinguish between two different dielectrophoretic regimes—positive (pDEP) and negative DEP (nDEP). pDEP occurs when the F_{CM} is greater than zero (which is a consequence of $\varepsilon_p^* > \varepsilon_m^*$) and particles are attracted to electric field intensity maxima and repelled from minima. Negative DEP occurs when the F_{CM} is less than zero (which implies the condition, $\varepsilon_p^* < \varepsilon_m^*$) and particles are attracted to electric field intensity minima and repelled from maxima. In pDEP, the force will be directed in the direction of the field gradient whereas in nDEP the force will be directed against the field gradient [16, 17].

Since the use of DEP to manipulate cells in microfluidics may involve the use of high local AC electric fields, it is important to the study whether these fields can have adverse effects on the cells [19]. At the frequencies used for electrical manipulation (1–25 MHz), the dominant interaction between the electrical field and the cell is via its internal cellular components [20]. A number of studies have shown that the exposure to the electrical fields applied to perform DEP can reach the levels required for electroporation and fusion of bacterial cells [21]. Furthermore, it has also been reported that DEP can allow the accurate manipulation of proteins forming the mitotic spindle in dividing mammalian cells without damaging them [22]. Research has been reported on genetic profiling analysis after DEP that suggests that DEP does not stress mammalian cells to the point that their viability is compromised [23]. Studies on yeast cell viability during the exposure to DEP have been reported [24]. Therefore, the current knowledge is that the DEP forces operate close to the limit of cell viability and it is a matter of debate whether the conditions used in DEP experiments might induce alteration in cell membrane potentials and structures, as well as in their internal metabolic machinery.

For microfluidic applications, it is important to evaluate the limiting conditions that can be used in terms of applied potential and flow rate in the microchannels that allow cell manipulation and assess their biocompatibility. In this work, pDEP and nDEP forces resulting from electric field gradients generated with a quadrupole design with no insulation layer are used to immobilize *Escherichia coli* cells in a PDMS microfluidic channel. The impact of DEP immobilization on cell viability is further studied using genetically modified *E. coli* cells to express green fluorescence protein (GFP) under the induction of IPTG. By monitoring the expression of the GFP reporter, we were thus able to confirm cell viability under flow conditions in a microfluidic environment by means of a metabolic outcome.

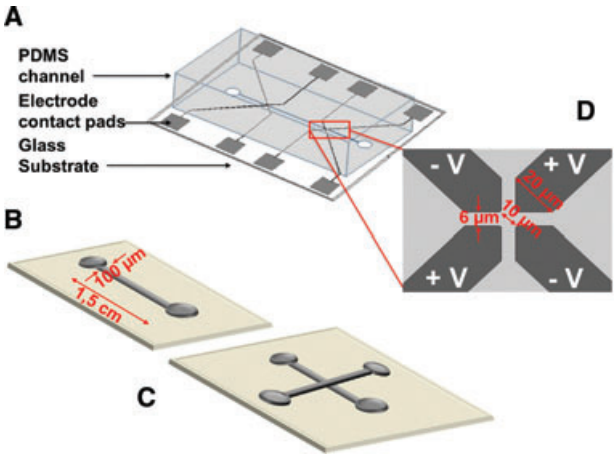

Figure 1. Microfluidic structure. (A) Integrated configuration, with a 7 µm high single PDMS microchannel (B) sealed to a glass substrate with patterned quadruple electrodes (D). (C) Double cross-shaped microchannel with the same dimension as of (B).

2 Materials and methods

2.1 Overall description

A PDMS microfluidic channel was sealed to a glass substrate with patterned titanium-tungsten electrodes (Fig. 1A). The PDMS channel (Fig. 1B and C) was fabricated by soft lithography using an SU-8 mould. A sinusoidal wave with frequency between 1 MHz to 25 MHz and peak-to-peak voltages in the range of 1–10 V_{pp} were applied to the electrodes using a signal generator (Agilent 3325, Agilent, OA, USA). The solutions were injected into the microchannels with a syringe pump (New Era Pump Systems) varying the fluid-flow velocity between 10×10^{-3} and 26×10^{-3} m/s. A fluorescence microscope (Leica DMLM) and a digital camera (Leica DFC300FX) were used for fluorescence and visible image acquisition and image analysis was performed using ImageJ (NIH) and Tracker (Video and Analysis Tool).

2.2 Electrodes fabrication

The electrodes were patterned on a glass substrate using a lift-off process. A positive photoresist (PFR 7790G27cP, JSR Electronics) was spin coated on the substrate and patterned by optical lithography (DWLii, HIMT, Heidelberg, Germany). After the photoresist was developed, 1500 Å of titanium-tungsten was deposited by reactive magnetron sputtering (Nordiko 7000). The sample was immersed in warm (65°C) photoresist solvent (Microstrip 2001, Arch Chemicals) to complete the lift-off process.

2.3 Microchannel fabrication and structure sealing

The following two designs of microchannels were used: a single microchannel (width, $W = 100$ μm, height, $H = 8$ μm, and length, $L = 1.5$ cm) (Fig. 1B); and a double microchannel composed of two crossed channels with the same dimensions (Fig. 1C). The channels were fabricated in PDMS using soft lithography. A negative mould of the PDMS microchannels was fabricated in 7 μm thick SU-8 2005 (Microchem Corp, MA, USA) photoresist on a crystalline silicon substrate. The SU-8 was patterned by exposure to UV light through an aluminum mask on a quartz substrate and developed with propylene-glycol-methyl-ether-acetate solution to remove the nonexposed SU-8. A 1:10 w/w mixture of curing agent and base PDMS (Sylgard 184) was dispensed on the mould and allowed to cure for 2 h at 70°C. The PDMS microchannel structure was manually peeled off from the SU-8 mould. The surfaces of the PDMS microchannels and the glass with patterned electrodes were exposed to 15 min of UV-ozone treatment (UVO cleaner 144AX, Jelight Company) for surface oxidation and cleaning. Finally, the channel and the electrodes were aligned under the microscope. The structure was left overnight to complete the irreversible sealing process.

2.4 Cell suspension and solution preparation

E. coli cells, approximately 1 μm of diameter, JM109 transformed with a pET28a + plasmid containing the GFP gene under an inducible lac promoter and the kanamycin resistance gene were used. IPTG (Fisher Scientific) was used to induce the expression of GFP. Cells were grown overnight at 37°C and 250 rpm in an orbital agitator using 5 mL of Tryptic Soy Broth (TSB, BD) medium (20 g/L TSB, no salt addition), 5 μL kanamycin, and 50 μL of *E. coli* stock. Cells were then harvested by centrifugation (4200 rpm for 10 min), washed, and resuspended in MilliQ water prior to insertion in the microfluidic system with a 5×10^6 cell m/L concentration.

Electrical conductivity measurements (conductivity tester OAKTON instruments) were performed for a range of dilutions of TSB and LB (Lysogeny broth, Sigma) mediums. Cell viability tests were performed with the Backlight kit (LIVE/DEAD® BacLight Bacterial Viability Kits, L7012) and trypan blue stain. All the dilutions mentioned in this work were made using MilliQ water (Merck, Millipore).

2.5 Modeling and simulation

Electric fields, DEP force, and fluid velocities were calculated using finite element analysis software (Comsol Multiphysics 3.5, Comsol). The module "AC/DC-electric quasistatics" and the "MEMS" module for microfluidics (using the incompressible Navier–Stokes approximation) were used for the physics subdomain settings in a 3D model. The electrical field was taken assuming only the maximum of the AC field over time, and the frequency dependence of the medium conductivity was used to obtain the F_{CM}. The F_{CM} was computed using

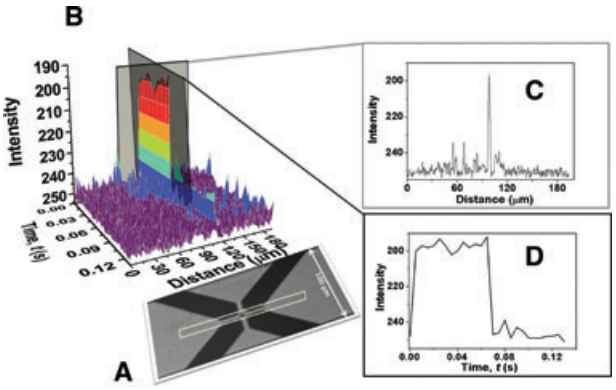

Figure 2. Image analysis of an nDEP experiment. A sinusoidal wave with 5 V_{pp} at 1 MHz was applied at $t = 0$ s and switched off at $t = 0.07$ s. (A) Eight-bit image from the sequential time stack. (B) Light intensity variation in the fixed area highlighted by a white rectangle in (A) during the experiment time 0–0.12 s. (C) Dependence of the intensity with distance at a fixed time, $t = 0.05$ s, highlighted in (A) by a light gray rectangle. (D) Dependence of the intensity with time for the fixed distance of 98 μm, highlighted in (A) by a dark gray rectangle.

MATLAB, assuming a rod-shape multishell model for a range of frequencies and media conductivities. Details of the models and numerical simulations can be found in Supporting Information Section 1 and Fig. 1.

2.6 Data acquisition and treatment

Visible and fluorescence microscopies were used to monitor cell trapping and GFP expression. In both cases, the image data were obtained in video format that was then converted into a stack of 8-bit images within a defined area around the trap (Fig. 2A). In visible microscopy, the quantification was made in terms of intensity, evaluated within the 8-bit gray scale, while in fluorescence microscopy the quantification was made assuming only the 8-bit image resultant from the RGB green component.

Each stack was analyzed for the area chosen and the data obtained were represented in 3D plot as shown in Fig. 2B. All values were normalized to the maximum of intensity achieved. The 3D plot is composed of the variation of intensity along the length of the defined area for a fixed time (Fig. 2C) and the time-dependent variation of intensity for a fixed location in the defined area (Fig. 2D). All intensity values, ranging from 0 to 255, were converted into percentage of black or white for the visible and fluorescence images, respectively. Details of the data treatment and acquisition can be found in Supporting Information Section 2.

3 Results and discussion

The conditions for DEP trapping of *E. coli* cells in a microfluidic channel were first estimated using a theoretical model and then experimentally studied as functions of the amplitude and frequency of the applied voltage, as well as

of the conductivity of the medium, in the absence of flow in the microchannel. The effect of the fluid-flow velocity on the DEP trapping efficiency was also studied. For an optimized set of DEP trapping conditions, in-flow metabolic viability tests were performed on *E. coli* cells during DEP force actuation in the microchannel.

3.1 Calculation of the effects of medium conductivity and frequency

The electrical conductivity of the growth media, TSB and LB, was studied for a range of dilutions (Supporting Information Fig. 2) in order to find the optimal dilution for pDEP or nDEP cell trapping. Figure 3A shows the real part of the F_{CM} calculated with the multishell cell model for a rod-shape live cell [18, 25], for different electrical conductivity values of the media (details of the model parameters are found in Supporting Information Section 1 and Table 1). Figure 3A shows that for lower conductivities (0.03 S/m), there is a transition between pDEP ($F_{CM} > 0$) and nDEP ($F_{CM} < 0$) at approximately 100 MHz. As the conductivity is increased to 0.35 S/m, the range of frequencies where pDEP can be achieved shrink, while for solutions with conductivities of 0.92 S/m only nDEP can be achieved.

Figure 3A shows that nDEP can be observed with a high value of F_{CM} approximately −0.5 (Table 1) using media with electrical conductivities of 0.92 S/m. However, these higher media conductivities cause electrode corrosion during field application. At a frequency of 1 MHz and using a medium with a lower electrical conductivity of 0.35 S/m, nDEP cell trapping with a F_{CM} of −0.3 is expected. This was the cell trap condition chosen for nDEP in this study as a compromise between the value of the generated DEP force and the electrode stability. For pDEP, a cell trap was chosen with a frequency of 15 MHz and a medium conductivity of 0.03 S/m, resulting in a F_{CM} of 0.6. This medium conductivity was chosen as it is low enough to allow a strong pDEP trap, but high enough to avoid ionic losses by the cells. The DEP force, calculated at the surface of the quadrupole electrodes, was simulated using Comsol Multiphysics 3.5 for the approximate values of F_{CM} of −0.3 for nDEP and 0.6 for pDEP (results shown in Supporting Information Fig. 3A–D). For pDEP, a maximum force is observed with absolute value of approximately 50 pN, while for nDEP, a maximum force of approximately 20 pN is calculated. For nDEP traps, the tendency is to trap cells in the minimum of the electric field gradient and, thus, the force is directed toward the center of the quadrupole electrodes. pDEP is characterized by cell attraction toward the areas where the electrical field gradient is maximum, thus, cells will be trapped between the arms of opposing electrodes.

3.2 Effect of the electric field and flow on DEP trapping

The sinusoidal voltage applied was varied from 1 to 10 V_{pp} using the nDEP (1 MHz, medium conductivity of 0.35 S/m) and pDEP (15 MHz, medium conductivity of 0.03 S/m) trapping conditions described above to concentrate *E. coli* cells in the microchannel with no flow. An increase in the trap intensity with electric field, followed by saturation, was observed for both nDEP and pDEP trapping conditions as shown in Fig. 3. An increase of the diameter of the trapped cell area with increasing electric field was observed for nDEP, while a poorer cell confinement with increasing values of V_{pp} was observed for pDEP. For nDEP conditions, no trapping was observed for V_{pp} <3 V (corresponding to an electric field of $\sim 3 \times 10^5$ V/m). Furthermore, the observed dependence of trapping on electric field was weaker than in the case of pDEP. Previous observations reported in the literature that suggested that nDEP traps did not show an increase of intensity and confinement with voltage increase [16] were thus not confirmed. Supporting Information Fig. 5 shows the dependence of the DEP force with the applied voltage at different heights in the microchannel, indicating a sharp decrease in force with increasing vertical distance from the electrodes.

For a cell suspension concentration of 5×10^6 cells m/L and in the absence of an electric potential, the trapped cells intensity is approximately 3 as indicated in Fig. 3A. Under nDEP conditions of 13×10^5 V/m, the intensity value increases to approximately 27 within the trap area. This intensity increase can be taken as corresponding to a fivefold increase in cell concentration due to DEP force. This is still an underestimation because the cell accumulation is expected to have a 3D configuration. Using the nDEP force calculated for a position 3 μm above the substrate, an *E. coli* cell that is approximately 30 μm from the center of the trap will experience a DEP force of approximately 6×10^{-12} N. This corresponds to a pulling movement toward the trap floor with a velocity of 3.18×10^{-4} m/s, as estimated using the Stokes drag force approximation. One can estimate that such a cell will take approximately 94 ms to reach the trap center. Assuming that the nDEP trapped cells collectively aggregate as a half sphere with a diameter of 4 μm (see Fig. 3B), and assuming an average volume of 2 μm^3 per cell, this corresponds to approximately 8–9 *E. coli* cells/trap.

The effect of combining DEP trapping and fluid flow in a microfluidic structure was also studied. The effect of the flow in the microchannel for different electric field values is shown for nDEP and pDEP traps in Supporting Information Fig. 4A and B, respectively. Cells under nDEP trapping conditions were confined to the trap until a maximum flow velocity of approximately 2.5×10^{-4} m/s. No significant intensity changes were observed for different fluid-flow velocities up to a critical value beyond which no trapping could be observed. As in the case of the no flow experiment shown in Supporting Information Fig. 4C, only very small changes in trapping efficiency were observed for different values of electric field under flow. For pDEP, cell trapping can be observed at higher flow rates up to 24×10^{-3} m/s (Supporting Information Fig. 4B). The absence of cell trapping for high fluid-flow velocities results from the fluid drag force overcoming the DEP force. The time taken for the nDEP intensity to saturate does not

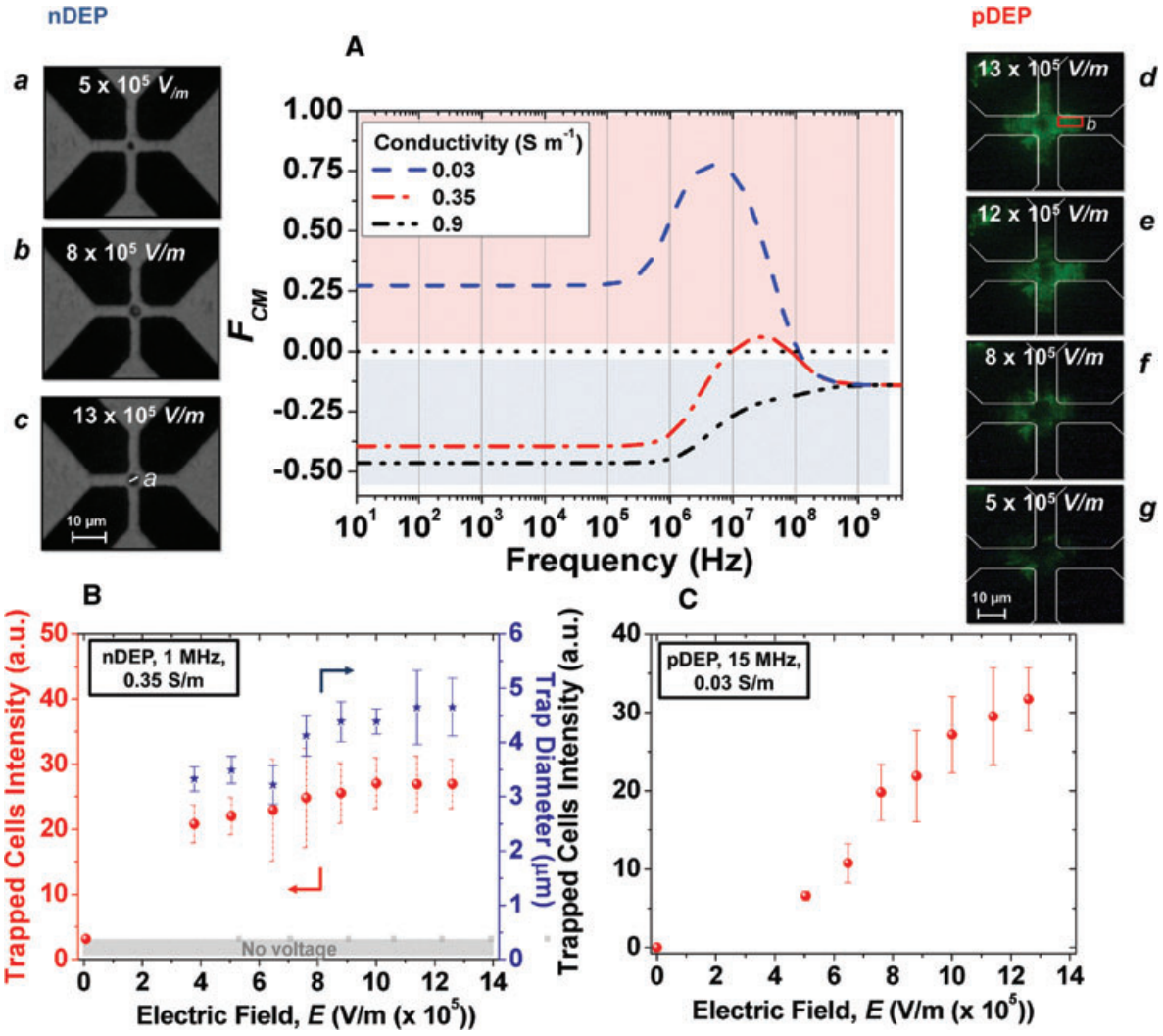

Figure 3. Effect of electric field on the number of live *E. coli* cells trapped, by nDEP and pDEP, in the microchannel in the absence of flow. (A) Real part of Clausius–Mossotti factor, for a rod-shape multishell cell model, calculated for media of different electrical conductivities. The positive region corresponds to pDEP and the negative region to nDEP conditions. (B) Intensity of trapped cells (bold circle) and diameter of the cell confinement area (bold triangle) for nDEP in TSB medium. Visible micrographs, (a)–(c), show the effect of the applied voltage on cell trapping at the center of the quadrupole and an example of the measurement of the diameter of the area of cell confinement (c). (C) The intensity of *Escherichia. coli* trapped for pDEP. Fluorescence micrographs, (d)–(g), show the confinement of GFP-expressing *E. coli* cells in the arms of the quadrupole with the area considered for the intensity measurements highlighted in red (*d*). Measurements were performed under conditions of no flow in the microchannel.

vary significantly with the fluid-flow velocity (Supporting Information Fig. 4C). The intensity of cells trapped by nDEP at 0.5 $\times$ 10^{-4} m/s is higher when compared with the values obtained for the conditions of zero flow or for higher fluid-flow velocities, whichever the applied voltages (Supporting Information Fig. 4C). This observation matches those made with single bead traps [26], and is not observed for pDEP cell trapping. In the experimental conditions discussed above, pDEP trapping forces are higher when compared with nDEP forces (in agreement with the information given in Fig. 3 and Supporting Information Fig, 3). This observation matches the observation that cells can be trapped by pDEP using significantly higher flow velocities in the microfluidic channel (of the order of 22 $\times$ 10^{-3} m/s, Supporting Information Fig. 4B). Supporting Information Fig. 6 equates the DEP force at different distances from the electrodes with the drag force that an *E. coli* cell is subject as calculated using the Stokes equation.

3.3 Dynamic exchange between trapped and flowing cells

During the in-flow cell trapping experiments described in Section 3.2 and Supporting Information Fig. 4, one question that arose was if there is a dynamic exchange regime between the DEP trapped cells and the cells flowing in the channel. To investigate this possibility, a trapping experiment

Table 1. Clausius–Mossoti factor, F_{CM}, for different media types and electrical conductivity used for different applied voltage frequencies

Media		F_{CM}		
Dilution factor	σ (S/m)	1 MHz	10 MHz	15 MHz
TSB 50×	0.03	0.538	0.732	0.662
TSB 6×	0.35	–0.280	0.127	0.155
LB 2×	0.92	–0.447	–0.269	–0.243

TSB, soybean casein digest medium; LB, lysogeny broth medium.

was designed using two distinct *E. coli* cell solutions: (i) in the first population no IPTG was added and so the cells did not produce GFP and, consequently, were not visible using fluorescence microscopy; (ii) in the second population IPTG was added during cell growth and the cells expressed GFP before being inserted in the microchannel. The experiment started by trapping cells of population (i) using nDEP (V_{pp} = 10 V at 1 MHz, 13 × 10^5 V/m). When the nDEP trap was filled, the flow of cells of population (i) was stopped, the channel was flushed, and cells of population (ii) were inserted at a velocity of approximately 6.3 × 10^{-5} m/s with a medium with an electrical conductivity of 0.35 S/m. This moment in time was taken as $t = 0$ s. Figure 4 shows that the fluorescence intensity in the trap region, which is zero at the start of the experiment, increases with time until reaching saturation at approximately 30 min indicating the trapping of cells of population (ii). Optical microscopy shows an approximately constant cell concentration in the trap indicating that the exchange of nonfluorescent cells of population (i) with fluorescent cells of population (ii) occurred within this time scale. The absolute value of the fluorescence indicates that only 50% of the original, nonfluorescent cells from population (i) were replaced by fluorescent cells from population (ii). Since the nDEP force decreases with the distance from the trap center (Supporting Information Figs. 3 and 5), it is hypothesized that the cell exchange occurred most likely between the loosely bound outer layers of the trapped cell agglomeration.

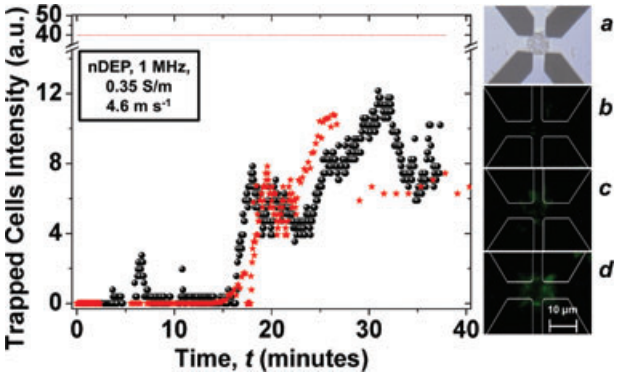

Figure 4. Dynamic exchange between trapped cells and cells flowing in the microchannel. nDEP-trapped cell intensity as monitored by fluorescence: the nDEP trap started with a trapped *E. coli* lineage that is not producing GFP (shown in (a) using optical microscopy) and then starting to flow, at time t = 0 min, a second *E. coli* lineage of cells that were expressing GFP. (b), (c), and (d) are fluorescence micrographs of the trap after 7, 19, and 33 min, of flow of GFP expressing cells, respectively. The total intensity of the trapped cells as monitored in the visible remained constant. Two independent repeats of the experiment are shown.

3.4 Trapped cell viability

The metabolic viability of cells during DEP trapping was studied by first performing a negative viability control with an *E. coli* population previously submitted to an ethanol shock for 30 min at 65 °C. These conditions effectively kill the cells, as confirmed using the trypan blue stain test. This group of dead cells was then inserted into the microchannel and subjected to the nDEP and pDEP conditions described in section 2.1. No trapping was observed in either case, since dead cells have different permittivities from their live counterparts. A second, positive test was performed by trapping cells under flow conditions using pDEP and testing for viability using the BacLight Bacterial Viability Kit. This kit makes use of two dyes to discriminate cells on the basis of the state of their membranes – cells with compromised membrane are stained red with ethidium bromide, whereas cells with intact membranes are stained green with Syto9. We observed (not shown) that trapped cells were green, suggesting that cells trapped by DEP were alive.

While the previous test indicates whether cells have their membrane intact or not, it gives no indication on their viability and activity in terms of metabolism. One way to study if cells are active in terms of their metabolism would be to induce GFP expression while the cells are trapped. To perform this test, noninduced *E. coli* cells were first trapped using nDEP in a single microchannel device (Fig. 1B). This cell culture (named population (i) in Section 3.3) was inserted without prior IPTG incubation. After successful trapping was confirmed using optical microscopy, an IPTG solution was immediately inserted in the microchannel (at time $t = 0$ indicated in Fig. 5). After approximately 14 min, fluorescence became detectable as shown in Fig. 5 (indicated by the open stars), demonstrating that the cells were expressing GFP and confirming the metabolic activity of the cells. A similar experiment was performed after trapping *E. coli* cells under pDEP conditions. The results were consistent with those obtained for nDEP, and an increase of fluorescence intensity was observed due to GFP expression after approximately 10 min of IPTG flow. In the above-described experiments, the same channel is used for cell and IPTG insertion and there is a possibility that the cells could be induced before reaching the trap area. To clarify this issue and in long nDEP experiments, the electrodes often become compromised, another pDEP experiment was performed in which a more complex two inlet microfluidic devices was used, one inlet for cell insertion and the other for the insertion of the IPTG solution. After

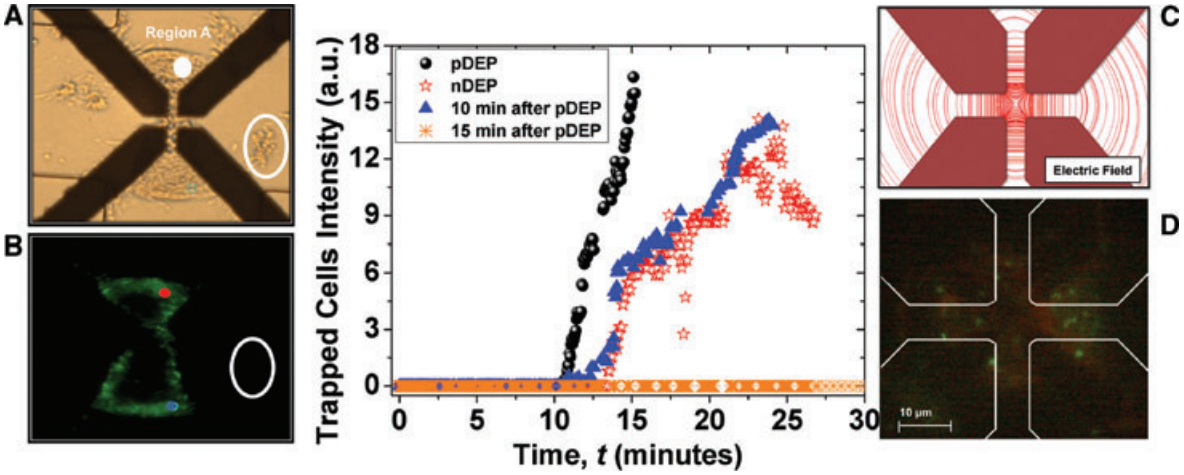

Figure 5. IPTG-induced GFP expression after nDEP and pDEP cell trapping. *E. coli* cells not producing GFP were trapped. In a first experiment, at $t = 0$ IPTG solution was inserted at 6.3×10^{-5} m/s for nDEP (open star) and 4.2×10^{-3} m/s/min for pDEP (bold circle). In a second experiment, IPTG was inserted at 0.2 μL/min after 10 min (bold triangle) and 15 min (asterisk) of pDEP trapping. (A) and (B) are optical and fluorescence micrographs, respectively, at the end of the first pDEP experiment. In the oval white selection there is a group of dead cells that do not express GFP upon IPTG induction. Electric field lines for 13×10^5 V/m (C). (D) Micrograph for viability test performed the second pDEP experiment (15 min of pDEP trapping prior to IPTG flow).

approximately 10 min, fluorescence became detectable as shown in Fig. 5 (indicated by the bold circles). In the case of this pDEP experiment, although Fig. 5A indicates that the trap is filled with cells, Fig. 5B shows that only the cells in the periphery of the trap, where the electric field gradient is lower, are expressing GFP. The electric field lines are schematically represented in Fig. 5C. The density of the lines is proportional to the field magnitude. This result suggests that the areas with higher forces due to the electric field gradient are not compatible with cell viability in this case (corresponding to regions where the electric field is higher than approximately 7×10^5 V/m, according to the simulations results). The shift between the onset of GFP expression, and thus of detection of fluorescence, between the nDEP and pDEP cell trapping conditions that can be observed in Fig. 5, could indicate an effect in nDEP of higher cellular stress induced by the heating of the solution due to the higher conductivity media employed, which delays GFP expression.

Additional experiments were performed to assess the metabolic viability of the cells subjected during different lengths of time to electric fields under pDEP and nDEP trapping conditions. Experiments analogous to those described above were performed, with the difference that the trapped *E. coli* cells were exposed to pDEP trapping fields for a further 10 and 15 min before initiating the flow of IPTG, and to nDEP trapping conditions for a further 5 min before IPTG. After this period, and keeping the applied fields on and the cells trapped, IPTG was introduced (6.3×10^{-5} m/s for nDEP and 4.2×10^{-3} m/s for pDEP). This set of experiments was performed using the cross-channel configuration. After 5 min of nDEP trapping, no fluorescence increase was observed upon IPTG induction. In the case of pDEP, an increase of induced fluorescence was observed for cells exposed for 10 min to the trapping fields. The induced fluorescence was observable after approximately 13 min of exposure to IPTG as shown in Fig. 5 (bold triangles). For cells exposed for 15 min to the trapping fields, no IPTG-induced fluorescence was detected up to 30 min of IPTG flow, as shown in Fig. 5 (asterisks). To evaluate if the cells were dead after 15 min of exposure to fields corresponding to the pDEP trapping conditions, a BacLight Bacterial Viability test was performed and red color was observed in the electrode area as depicted in Fig. 5D indicating cell death. Comparing the cells exposed to pDEP conditions for 10 min to those for which IPTG was introduced immediately after trapping, Fig. 5 shows that the onset of GFP expression is earlier, and higher expression slope and expression levels are observed for the cells exposed to the DEP electric fields for shorter times. From these results, one can conclude that the cell metabolism is affected by the DEP trapping fields after 10 min of exposure, while after 15 min of exposure the cells no longer produce GFP, the majority being dead. pDEP is suitable to manipulate cells for a short period of time without compromising their metabolic viability, but long exposures to the DEP electric fields can be harmful.

4 Concluding remarks

This work demonstrated that *E. coli* cells trapped in a microchannel either using either pDEP or nDEP under conditions of fluid flow remain viable and able to use their biomolecular machinery to produce proteins (GFP). To achieve this result, the DEP forces resulting from an integrated quadrupole electrode were simulated and the experimental predictions were confirmed both in the absence and in the presence of flow in microchannels. Beyond a certain electrical field magnitude (~13×10^5 V/m) and 15 min

of pDEP-exposure time, the viability of the cells was shown to be compromised. Meanwhile, after 10 min of pDEP exposure time in the same conditions, the cell viability was confirmed.

These results provide important guidance for the development of a number of lab-on-chip applications: (i) the observed effect of cell concentration can potentially be used to increase the sensitivity of integrated biosensors and the speed of miniaturized bioanalysis; (ii) the metabolic viability of trapped cells suggests that genetically modified trapped cells can be used as live biosensors in which the timing and amplitude of the expression of a marker protein can be correlated with a complex fluidic stimulation; and (iii) the robust definition of trapping conditions, in particular, the time of exposure to the electric field, and the observation that dead cells are not trapped indicates that complex spatial and chemical manipulation of cells can be performed in microfluidic devices without compromising cell viability.

This work was supported by Fundação para a Ciência e a Tecnologia (FCT) through research project Micro 2D-FS (PTDC/CTM/104387/2008). The authors also acknowledge funding from FCT through the Associated Laboratories IN—Institute of Nanoscience and Nanotechnology and IBB—Institute of Biotechnology and Bioengineering.

The authors have declared no conflict of interest.

5 References

[1] Edwards, C., *Environmental Monitoring of Bacteria*, Humana Press, Totowa, 1999.

[2] Girotti, S., Ferri, E. N., Fumo, M. G., Maiolini, E., *Anal. Chim. Acta* 2008, *608*, 2–29.

[3] deMello, A. J., *Nature* 2006, *442*, 394–402.

[4] Yager, P., Edwards, T., Fu, E., Helton, K., Nelson, K., Tam, M. R., Weigl, B. H., *Nature* 2006, *442*, 412–418.

[5] Janasek, D., Franzke, J., Manz, A., *Nature* 2006, *442*, 374–380.

[6] Yu, Z. T. F., Kamei, K., Takahashi, H., Shu, C. J., Wang, X., He, G. W., Silverman, R., Radu, C. G., Witte, O. N., Lee, K.-B., Tseng, H.-R., *Biomed. Microdevices* 2009, *11*, 547–555.

[7] Escarpa, A., González, M. C., Gil, L., Angel, M., Crevillén, A. G., Hervás, M., García, M., *Electrophoresis* 2009, *29*, 4852–4861.

[8] Yang, F., Yang, X., Jiang, H., Bulkhaults, P., Wood, P., Hrushesky, W., Wang, G., *Biomicrofluidics* 2010, *4*, 013204.

[9] Becker, F. F., Wang, X. B., Huang, Y., Pethig, R., Vykoukal, J., Gascoyne, P. R., *Proc. Natl. Acad. Sci. USA* 1995, *92*, 860–864.

[10] Sia, S. K., Whitesides, G. M., *Electrophoresis* 2003, *24*, 3563–3576.

[11] Gardeniers, H., Van Den Berg, A., *Int. J. Environ. Anal. Chem.* 2004, *84*, 809–819.

[12] Rothert, A., Deo, S. K., Millner, L., Puckett, L. G., Madou, M. J., Daunert, S., *Anal. Biochem.* 2005, *342*, 11–19.

[13] Pethig, R., *Biomicrofluidics* 2010, *4*, 039901.

[14] Gascoyne, P. R. C., Vykoukal, J., *Electrophoresis* 2002, *23*, 1973–1983.

[15] Suehiro, J., Hamada, R., Noutomi, D., Shutou, M., Hara, M., *J. Electrostat.* 2003, *57*, 157–168.

[16] Voldman, J., in: Ferrari, M., Bashir, R., Wereley, S. (Eds.), *BioMEMS and Biomedical Nanotechnology*, Springer US, Boston, MA 2011, pp. 159–186.

[17] Pohl, H., *Dielectrophoresis: the Behavior of Neutral Matter in Nonuniform Electric Fields*. Cambridge University Press, Cambridge, New York 1978.

[18] Jones, T. B., *Electromechanics of Particles*. Cambridge University Press, New York, 2005.

[19] Yang, L., Banada, P. P., Bhunia, A. K., Bashir, R., *J. Biol. Eng.* 2008, *2*, 6.

[20] Cooper, G. M., Hausman, R. E., *The Cell: a Molecular Approach*, 5th Edn., Sinauer Associates, Washington, 2009.

[21] Oblak, J., Krizaj, D., Amon, S., Macek-Lebar, A., Miklavcic, D., *Bioelectrochemistry* 2007, *71*, 164–171.

[22] Uppalapati, M., Huang, Y.-M., Aravamuthan, V., Jackson, T. N., Hancock, W. O., *Integr. Biol.* 2011, *3*, 57–64.

[23] Huang, Y., Joo, S., Duhon, M., Heller, M., Wallace, B., Xu, X., *Anal. Chem.* 2002, *74*, 3362–3371.

[24] Arnold, W. M., Franich, N. R., *Curr. Appl. Phys.* 2006, *6*, 371–374.

[25] Castellarnau, M., Errachid, A., Madrid, C., Juarez, A., Samitier, J., *Biophys. J.* 2006, *91*, 3937–3945.

[26] Voldman, J., Braff, R. A., Toner, M., Gray, M. L., Schmidt, M. A., *Biophys. J.* 2001, *80*, 531–541.

